THE JOURNAL OF PHYSICAL CHEMISTRY A

Article

pubs.acs.org/JPCA

Infrared Photodissociation Spectroscopy of Microhydrated Nitrate–Nitric Acid Clusters $NO_3^-(HNO_3)_m(H_2O)_n$

Nadja Heine,[†] Tara I. Yacovitch,[‡] Franziska Schubert,[†] Claudia Brieger,[†] Daniel M. Neumark,*[,‡,∥] and Knut R. Asmis*[,†,§]

[†]Fritz-Haber-Institut der Max-Planck-Gesellschaft, Faradayweg 4-6, D-14195 Berlin, Germany

[‡]Department of Chemistry, University of California, Berkeley, California 94720, United States

[§]Wilhelm-Ostwald-Institut für Physikalische und Theoretische Chemie, Universität Leipzig, Linnéstrasse 2, D-04103 Leipzig, Germany

[∥]Chemical Science Division, Lawrence Berkeley National Laboratory, Berkeley, California 94720, United States

Supporting Information

ABSTRACT: Infrared multiple photon dissociation (IRMPD) spectra of $NO_3^-(HNO_3)_m(H_2O)_n(H_2)_z$ with m = 1–3, up to n = 8 and $z \geq 1$, are measured in the fingerprint region (550–1880 cm^{-1}), directly probing the NO-stretching modes, as well as bending and other lower frequency modes. The assignment of the spectra is aided by electronic structure calculations. The IRMPD spectrum of the m = 1, n = 0 cluster is distinctly different from all the other measured spectra as a result of strong hydrogen bonding, leading to an equally shared proton in between two nitrate moieties ($O_2NO^-\cdots H^+\cdots ONO_2^-$). It exhibits a strong absorption at 877 cm^{-1} and lacks the characteristic NO_2-antisymmetric stretching/NOH-bending mode absorption close to 1650 cm^{-1}. Addition of at least one more nitric acid molecule or two more water molecules weakens the hydrogen bond network, breaking the symmetry of this arrangement and leading to localization of the proton near one of the nitrate cores, effectively forming HNO_3 hydrogen-bonded to NO_3^-. Not all IR active modes are observed in the IRMPD spectra of the bare nitrate–nitric acid clusters. Addition of a water or a hydrogen molecule lowers the dissociation limit of the complexes and relaxes (H_2O) or lifts (H_2) this IRMPD transparency.

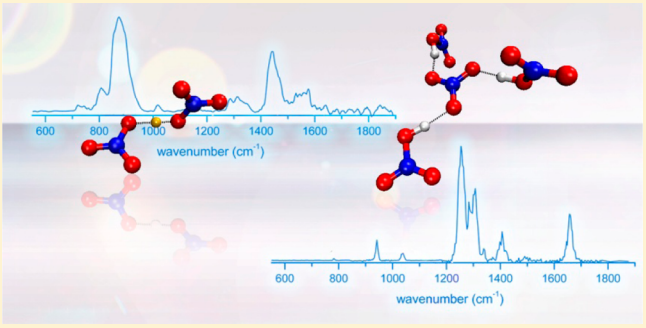

I. INTRODUCTION

Nitrate-containing ions play an important role in chemical and physical processes in the atmosphere, such as electrical conductivity and the formation of new particles through ion nucleation.[1,2] Nitrate (NO_3^-) and its clusters with nitric acid (HNO_3) and water are among the most abundant anions in the atmosphere. They were first measured in the stratosphere in 1978[3] and, five years later, in the troposphere by Arnold with a balloon-borne mass spectrometer.[4] While $NO_3^-(HNO_3)_2$ accounts for over 90% of all negative ions at heights around 27–30 km,[5] $NO_3^-(HNO_3)(H_2O)$ dominates in the tropospheric regions, due to a higher abundance of water vapor.[6] A major source of these clusters is oxidation of NO_x to HNO_3 and subsequent deprotonation via galactic cosmic rays, radioactivity, and electrical discharges.[1] The resulting NO_3^- reacts promptly with trace gases via ion–molecule reactions forming $NO_3^-(HNO_3)_m(H_2O)_n$ clusters. Understanding the structure, stability, reactivity, and growth rates of nitrate-containing clusters is crucial for improving atmospheric ion chemistry models.[7] Here, we use vibrational spectroscopy of gas phase cluster anions in combination with electronic structure calculations to investigate the geometric structure and stability of $NO_3^-(HNO_3)_m(H_2O)_n$ clusters with m = 1–3 and up to n = 8, in order to complement mass spectrometric and kinetics experiments and to test structural predictions from earlier computational studies.[8,9]

Previous experimental[10−13] and theoretical[14,15] studies have mainly focused on the m = 1, n = 0 cluster, also referred to as hydrogen dinitrate ($O_2NO^-\cdots H^+\cdots ONO_2^-$), due to the presence of an equally shared proton as a consequence of strong hydrogen bonding.[16] A variety of salts has been investigated with X-ray and neutron diffraction,[17,18] as well as infrared (IR)[19] and resonance Raman spectroscopy,[20] showing that the nominally planar and centrosymmetric D_{2h} structure can be distorted depending on the counterions. Rate constants, reaction enthalpies, and bond energies have been determined experimentally for $NO_3^-(HNO_3)_m(H_2O)_n$ using mass spectrometry, in order to investigate the process of dissociation/formation.[21−24] These experiments show similar clustering behavior as was recently

Special Issue: Kenneth D. Jordan Festschrift

Received: December 13, 2013
Revised: March 25, 2014
Published: March 25, 2014

dx.doi.org/10.1021/jp412222q | J. Phys. Chem. A 2014, 118, 7613–7622

reported for sulfate/sulfuric acid/water clusters:[25] the formation of $A^-(HA)_{1-3}$ with A = HSO_4^- or NO_3^- is preferred over $A^-(H_2O)$ because the acid molecule binds more strongly to the conjugate base anion than the water molecule. For example, in the reaction $NO_3^-{\cdot}H_2O + HNO_3 \rightarrow NO_3^-{\cdot}HNO_3 + H_2O$ ($k = 5.5 \times 10^{-10}$ cm^3/s), water is rapidly replaced by nitric acid.[21] The experimentally determined sequential enthalpies of complexation for 1−3 molecules of HNO_3 to NO_3^- are −113, −67, and −54 kJ/mol, respectively; these relatively high values indicate strong association complexes of nitric acid with nitrate.[26,27] The most extensive *ab initio* calculations on $NO_3^-(HNO_3)_m$ with m = 1−3 have been performed by Galvez et al.[9] They found planar global minimum-energy structures for all three clusters and nonplanar relative minima only slightly higher in energy. For m > 1, they predicted a distortion of the symmetric $O_2NO^-\cdots H^+\cdots ONO_2^-$ arrangement, leading to asymmetric $O_2NO^-\cdots H-ONO_2(HNO_3)_{m-1}$ structures as the hydrogen bond (HB) network grows in the cluster.

In a previous IRMPD study on microhydrated $NO_3^-(H_2O)_{1-6}$ clusters,[28] it was demonstrated that the degeneracy of the antisymmetric NO_3^- stretching vibration ν_3 can be exploited as a sensitive indicator for the symmetry of the microhydration shell/HB network and that NO_3^- favors surface hydration, in contrast to the internal solvation of sulfate dianions.[29,30] Recent studies on mixed bisulfate/nitrate/neutral acid clusters explored the influence of acid solvation on the conjugated base anion and not only showed that the charge localization can vary unexpectedly upon cluster composition, but also revealed the sensitivity of the NO_2-antisymmetric stretching/NOH-bending mode to the presence of an intact HNO_3 molecule.[31] Studies on bisulfate/sulfuric acid clusters demonstrated that certain normal modes, mainly those that are localized on the HB network, show a large degree of IRMPD transparency.[25] Upon messenger-tagging with H_2, the linear IR intensity of these modes was recovered, since photodissociation can then occur immediately upon the absorption of a single photon.

The present investigation of the structure and energetics of nitrate/nitric acid/water clusters is aimed at ultimately shedding new light on the early steps in the formation of nitric acid aerosols. Here, we present IRMPD spectra of these mass-selected clusters from 550 to 1880 cm^{-1}, the spectral region covering the vibrational modes of the nitrate ion and characteristic modes of the solvent molecules. When possible, we use messenger-tagging with H_2 to probe the linear absorption spectra. The vibrational spectra are assigned to a particular structure or family of structures based on a comparison to simulated IR spectra from electronic structure calculations. Our analysis shows that the first water molecule does not disturb the shared proton motif of the m = 1 cluster, but additional solvent molecules disrupt the symmetric arrangement.

II. EXPERIMENTAL AND THEORETICAL METHODS

The IRMPD experiments were carried out using a previously described ion-trap tandem-mass-spectrometer,[32,33] which was temporarily installed at the "Free Electron Laser for Infrared eXperiments" (FELIX) user facility[34] at the FOM Institute Rijnhuizen (Nieuwegein, The Netherlands). Briefly, microsolvated nitrate/nitric acid clusters, $NO_3^-(HNO_3)_m(H_2O)_n$, are produced by electrospray in a modified commercial Z-spray source from a 10 mM solution of HNO_3 in a 1:1 water/acetonitrile solvent mixture. The beam of ions is skimmed and collimated in a decapole ion guide, and subsequently mass-selected in a commercial quadrupole mass filter. After mass selection, the cluster anions are deflected by 90° using an electrostatic quadrupole deflector and focused into a cryogenically cooled ion trap, held at 10 K. Here, the anions are collected for 99 ms and thermalized through collisions with a buffer gas (He/H_2). In a 10 Hz cycle, ions are extracted and focused into the center of the extraction region of a time-of-flight mass spectrometer, where they interact with a single FELIX macropulse. If the wavelength of the IR radiation is in resonance with a vibrational transition, fragmentation of the (parent) cluster anions occurs. All anions are extracted by a set of high voltage pulses and are detected as a function of their flight time using an MCP detector. Photodissociation spectra in the linear absorption regime are obtained by condensing molecular hydrogen onto the mass-selected cluster anions in the ion trap. The photodissociation cross section σ_{IRMPD} is determined from the relative abundances of the parent and photofragment ions, $I_P(\nu)$ and $I_F(\nu)$, and the frequency-dependent energy fluence (assuming a constant interaction area throughout the range of scanned wavelengths) $\varphi_e(\nu)$ using[35]

$$\sigma_{IRMPD} = -\ln\left[1 - \frac{I_F(\nu)}{I_P(\nu) + I_F(\nu)}\right]/\varphi_e(\nu)$$

When investigating tagged species, we assume a single-photon process. Intensities are therefore normalized to the photon fluence,[36] $\varphi(\nu) = \varphi_e(\nu)/h\nu$, such that $\sigma \propto \sigma_{IRMPD}\nu$.

In order to support the analysis of the experimental spectra, DFT calculations were performed using the TURBOMOLE program package.[37−39] The B3LYP hybrid functional[40−42] (gridsize m5) is employed in combination with Dunning aug-cc-pVTZ basis sets.[43] Structure optimizations use tight convergence criteria, Cartesian gradients smaller than 1×10^{-4} Hartree/Bohr, and energy changes smaller than 1×10^{-6} Hartree; see Supporting Information (SI) for total energies. The SCF convergence criterion is 1×10^{-7} Hartree for the energy and 1×10^{-7} a.u. for the root-mean-square of the density. Harmonic vibrational frequencies are obtained from second analytic derivatives.[44] It is known that B3LYP vibrational frequencies are systematically too large (see, e.g., refs 45,46). Agreement with observed frequencies can be improved by scaling, which accounts for neglected anharmonicities as well as systematic errors of the calculated harmonic force constants. We use 0.968 as a scaling parameter, which falls into the known ranges for the B3LYP functional.[45,46]

III. RESULTS

Trends in Experimental IRMPD Spectra. Overviews of the IRMPD spectra of $NO_3^-(HNO_3)_m(H_2O)_n(H_2)_z$ clusters in the fingerprint region (530−1880 cm^{-1}) are shown in Figures 1 and 2. The stoichiometry of the clusters is abbreviated by (m,n,z). The spectra of the m = 1−3 clusters without water (n = 0) are compared to the thin film IR-spectrum of pure HNO_3,[47] measured at 45 K, in Figure 1. The spectra are arranged from top to bottom according to increasing number of neutral acid molecules. The hydrogen-tagged equivalents, when available, are shown above the IRMPD spectrum of the corresponding bare cluster anion. Spectral features are labeled with **A**, **B**, and **P** according to their assignment to modes of nitric acid molecules (**A**), those of the conjugate base nitrate anion (**B**), and to shared proton (**P**) modes. The detailed assignments, described in the Analysis section, together with experimental and calculated band positions, are listed in Table 1. The band assignments are derived

dx.doi.org/10.1021/jp412222q | J. Phys. Chem. A 2014, 118, 7613−7622

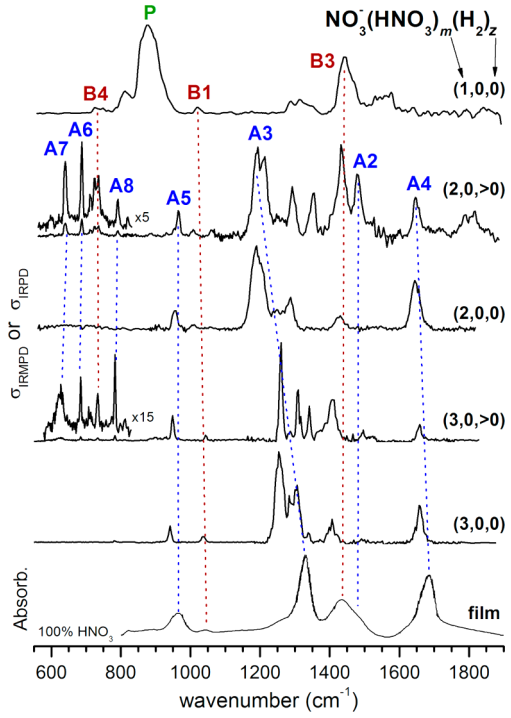

Figure 1. Experimental IRMPD spectra of $NO_3^-(HNO_3)_m(H_2O)_n(H_2)_z$ clusters with m = 1−3 and n = 0 abbreviated as (m,n,z). Peaks are labeled according to their assignment to modes of the neutral acid molecule (**A**), of the conjugate base anion (**B**), or to the shared proton stretching mode (**P**). See Table 1 also for peak positions and assignments.

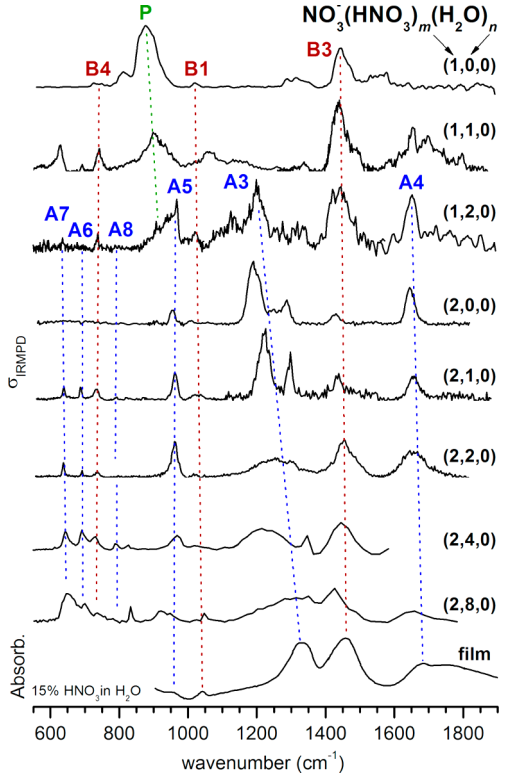

Figure 2. Experimental IRMPD spectra of $NO_3^-(HNO_3)_m(H_2O)_n(H_2)_z$ clusters with m = 1,2, n = 1−8, z = 0 (top panels) compared to absorption spectra[47] of amorphous 15% HNO_3 in H_2O. Peaks are labeled according to their assignment to modes of the neutral acid molecule (**A**), of the conjugate base anion (**B**), or to the shared proton stretching mode (**P**).

from the local modes (see Table 2) of the bare nitrate ($^B\nu_1$ − $^B\nu_4$), nitric acid ($^A\nu_1$ − $^A\nu_9$), and the shared proton ($^P\nu_{x,y,z}$).

In the following description of the experimental IRMPD spectra, we will first focus on identifying general trends. The spectral features are tentatively assigned based on a comparison to previous IRMPD results on related systems[25] as well as IR and Raman measurements of solid complexes,[11] matrix-isolated species,[48] condensed phase samples,[47,49] and nitric acid vapor.[50] This preliminary assignment is then evaluated in more detail in the Analysis section, where we compare the experimental data to simulated IR spectra.

The IRMPD spectra presented in Figure 1 show a rich structure of IR active peaks of varying widths and positions. Several general trends are observed. First, the H_2-tagged spectra show the most bands and these are typically narrower than their counterparts in the IRMPD spectra. The absence of IR bands in the spectra of the untagged anions is reminiscent of observations made in the IRMPD study on bisulfate/sulfuric acid/water clusters,[25] where it was discussed in terms of "IRMPD transparent" modes, although the origin of this IRMPD transparency is slightly different here (see Discussion). Second, the IRMPD spectrum of (1,0,0) is characteristically different from the spectra of the larger clusters, suggesting a significantly different binding motif in this cluster. IR and Raman studies of solid m = 1, n = 0 complexes[11,48] find evidence for exceptionally strong hydrogen bonds and a dramatically red-shifted hydrogen bonded O−H stretching mode (~600 cm^{-1}), indicative of a hydrogen dinitrate species containing a shared proton. The IR spectrum of (1,0,0) indeed exhibits an intense band at 877 cm^{-1} (**P**), not observed in the spectra of the larger clusters, and we therefore attribute band **P** to the shared-proton stretching mode in $O_2NO^-\cdots H^+\cdots ONO_2^-$.

Most of the other observed spectral features in Figure 1 can be assigned to characteristic absorptions of nitrate ions and nitric acid molecules by comparison to previous experiments. The four normal modes of nitrate (see Table 2) have been observed at 1404/1348 ($^B\nu_3$), 1049 ($^B\nu_1$), 825 ($^B\nu_2$), and 719 cm^{-1} ($^B\nu_4$) in liquid alkali nitrate solution.[49] Here, the $^B\nu_3$ mode, the nominally doubly degenerate and intense antisymmetric stretch of the NO_3^- moiety, splits into two components due to asymmetric solvation. Previous experiments on NO_3^-·Ar in the gas phase[51] showed that this splitting is not seen in the absence of perturbing solvent molecules. The IR photodissociation spectrum of NO_3^-·Ar is therefore characterized by a single, intense band, observed at 1349 cm^{-1}.[51] In our spectra, signal attributed to three of these modes ($^B\nu_3$, $^B\nu_1$, and $^B\nu_4$) is observed and correlates to the bands labeled **B3** (1437 cm^{-1}), **B1** (1015 cm^{-1}), and **B4** (725 cm^{-1}), respectively. As will be shown later, the $^B\nu_3$ modes of both nitrate moieties actually couple strongly, leading to the observed splitting into the three groups of peaks in between 1250 and 1600 cm^{-1}.

Four modes of neutral nitric acid molecules can be assigned by comparison with the data from IR measurements on thin films of pure HNO_3 (see lowest spectrum labeled "film" in Figure 1).[47] The NO_2 antisymmetric stretch ($^A\nu_4$), N−O−H bend ($^A\nu_2$), NO_2 symmetric stretch ($^A\nu_3$), and the N−O(H) stretch ($^A\nu_5$) are located at 1686, ~1480, 1328, and 965 cm^{-1} in the condensed phase spectrum, and the corresponding bands in our gas phase spectra are labeled with **A4**, **A2**, **A3**, and **A5**. The nitric acid core

dx.doi.org/10.1021/jp412222q | J. Phys. Chem. A 2014, 118, 7613−7622

Table 1. Experimental and Calculated Band Positions (in cm^{-1}) of $NO_3^-(HNO_3)_m$ Clusters with $m = 1-3$[a]

	$m = 1$					$m = 2$			$m = 3$		
band	Exp.	1w0a[b]	Mode	1w0b[b]	Mode	Exp.	2w0a[b]	Mode	Exp.	3w0a[b]	Mode
A4						1647	1629	$^A\nu_4$, $^A\nu_2$	1658	1635	$^A\nu_4$, $^A\nu_2$
A2						1478	1439	$^A\nu_2$, $^A\nu_4$	1409	1397	$^A\nu_2$, $^A\nu_4$
B3″	1554			1490	$^B\nu_3$, $^P\nu_x$						
B3	1437	1422	$^B\nu_3$, $^P\nu_y$	1401	$^B\nu_3$, $^P\nu_y$	1432	*1393*	$^B\nu_3$	1341	1359	$^B\nu_3$
B3′	1330			1319	$^B\nu_3$, $^P\nu_z$	1355	1322	$^B\nu_3$, $^A\nu_3$	1310	1347	$^B\nu_3$
A3′						1292	1288	$^A\nu_3$			
A3						1193	1224	$^A\nu_3$, $^B\nu_3$	1261	1269	$^A\nu_3$
A9′	~1162	1186	$^P\nu_z$			1059					
A9						1008	1025	$^A\nu_9$			
B1	1015	1053	$^B\nu_1$, $^P\nu_x$	1045	$^B\nu_1$, $^P\nu_x$				1043	1053	$^B\nu_1$
A5						964	*946*	$^A\nu_5$	949	932	$^A\nu_5$
P	877	919	$^P\nu_x$, $^B\nu_4$	868	$^P\nu_x$, $^B\nu_4$						
A8						791	780	$^A\nu_8$	783	775	$^A\nu_8$
B4	725	711	$^B\nu_4$, $^P\nu_x$	709	$^B\nu_4$, $^P\nu_y$	723,736	704	$^B\nu_4$	734	717	$^B\nu_4$
A6						687	674	$^A\nu_6$	684	669	$^A\nu_6$
A7						640	631	$^A\nu_7$	627	623	$^A\nu_7$

[a]The experimental band positions are determined from the IRMPD spectra shown Figure 1. The calculated positions are determined from the simulated B3LYP/aug-cc-pVTZ IR-spectra of the lowest energy isomers shown in Figures 3−5. Vibrational modes (ν) are numbered and labeled with **A**, **B**, and **P** according to their assignment to the normal modes of the nitric acid molecule (**A**), of the conjugate base nitrate anion (**B**), or of the shared proton (**P**) (see Table 2). [b]See Figures 3−5 for the corresponding structures of the listed isomers and Table 3 for the relative energies.

Table 2. Labeling, Description, and Experimental Values (in cm^{-1}) of the Normal Modes of the Nitric Acid Molecule (HNO_3) and the Nitrate Anion (NO_3^-)

nitric acid molecule (A)			nitrate anion (B)		
mode	description	exp.	mode	description	exp.
$^A\nu_1$	O−H stretch	3550[a]	$^B\nu_1$	NO sym. stretch	1049[c]
$^A\nu_2$	NO_2 antisym. stretch	1710[b]	$^B\nu_2$	Out-of-plane deformation	825[c]
$^A\nu_3$	NO_2 sym. stretch	1331[a]	$^B\nu_3$	NO antisym. stretch	1349[d]
$^A\nu_4$	H−O−N bend	1325[a]	$^B\nu_4$	in-plane rock	719[c]
$^A\nu_5$	(H)O−N stretch	879[a]			
$^A\nu_6$	NO_2 scissor	647[a]			
$^A\nu_7$	(H)O−N−O bend	579[a]			
$^A\nu_8$	NO_2 wag	762[a]			
$^A\nu_9$	HONO torsion	456[a]			

[a]Gas phase. ref 50. [b]Gas phase. ref 62. [c]Solution. ref 49. [d]Gas phase. ref 51.

bends $^A\nu_{6-8}$ (550−791 cm^{-1}) are known from IR absorption spectra of nitric acid vapor (579−762 cm^{-1}),[50] as well as in a N_2 matrix (597−767 cm^{-1}),[48] and correlate with bands **A6** to **A8**.

We also measured IRMPD spectra of partially hydrated nitrate/nitric acid clusters for $m = 1$ and $m = 2$. These are shown in Figure 2, where they are also compared to the thin film IR-spectrum of a HNO_3/H_2O binary amorphous mixture containing predominantly dissociated acid molecules. For $m = 1$, addition of a single water molecule to hydrogen dinitrate leads to partial lifting of some of the IRMPD transparent modes (see Analysis), but otherwise perturbs the band positions in the IR spectrum rather weakly. Solvation by at least two water molecules or another nitric acid molecule, on the other hand, leads to more significant changes in the IRMPD spectrum, namely, the appearance of the intense bands **A3** and **A5** and the disappearance of the shared-proton stretching mode **P**. For $m = 2$, the addition of a single water molecule is sufficient to recover the IRMPD transparent modes **B4** and **A6-A8** in the core bend region ($\lesssim$850 cm^{-1}). The most striking change in the gas phase spectra upon hydration with up to eight water molecules is the blue shift of band **A3** from 1190 cm^{-1} in the (2,0,0) spectrum to above 1300 cm^{-1} in the (2,8,0) spectrum, indicating a strengthening of the nitric acid N=O bonds upon hydration. Moreover, band **B3**, associated with the antisymmetric stretch of the nitrate anion, increases in relative intensity upon micro-hydration, while the bands attributed to intact nitric acid decrease. Comparison of the thin film IR spectrum to the gas phase IRMPD-spectrum of (2,8,0) in Figure 2 shows that most absorption features have nearly converged toward the condensed phase limit with regard to position and width. Hence, the formation of a local hydrogen bond network is mainly responsible for the increase in width of the absorption features and already quite reasonably reproduced by the addition of a few water molecules ($n \geq 4$) to $NO_3^-(HNO_3)_2$.

IV. ANALYSIS

The experimental IRMPD spectra of the nitrate/nitric acid/water clusters are compared to simulated IR spectra derived from harmonic frequencies and intensities in Figures 3−5, respectively. Band positions and scaled harmonic frequencies as well as an approximate normal mode description are listed in Table 1. Table 3 gives an overview of relative energies and symmetries of the discussed isomers. The H_2-tagged spectra are shown at the top of each figure that includes tagged results, followed by the IRMPD spectrum of the bare cluster and then the spectra of the microhydrated clusters with increasing number of water molecules. For each cluster, two simulated spectra are shown. Minimum-energy geometries are shown alongside the figures, labeled according to cluster size, number of water molecules, and energetic ordering (e.g., a, b, ...). For instance, **1w0a** refers to the lowest energy structure of the $m = 1$, $n = 0$ cluster. A complete list of all calculated structures, their relative energies, and simulated IR spectra is found in the SI.

dx.doi.org/10.1021/jp412222q | J. Phys. Chem. A 2014, 118, 7613−7622

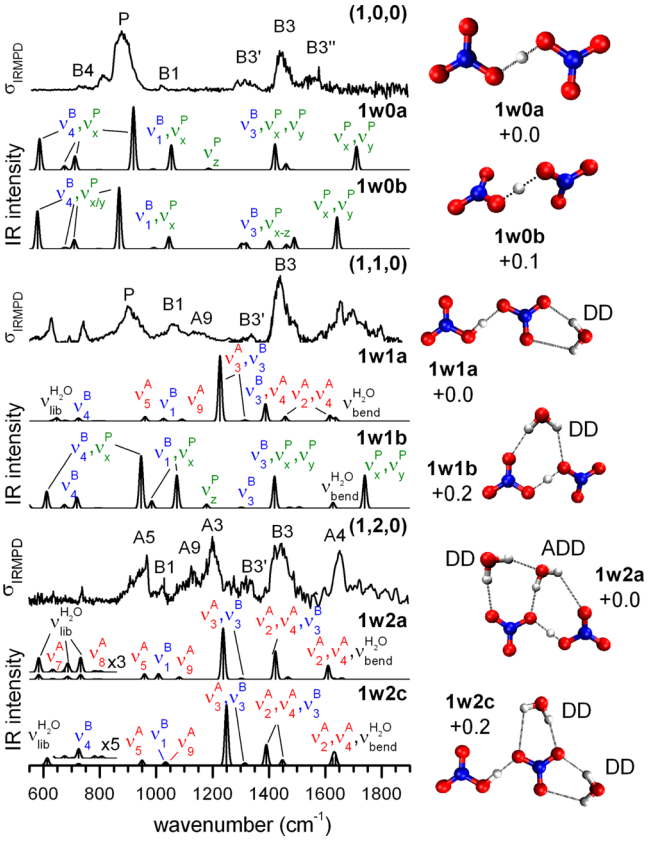

Figure 3. Experimental IRMPD and simulated linear absorption spectra of $NO_3^-(HNO_3)_m(H_2O)_n(H_2)_z$ complexes, abbreviated by (m,n,z), for $m = 1$, $z = 0$. Simulated spectra, derived from B3LYP/aug-cc-pVTZ scaled (0.968) harmonic frequencies and intensities, are convoluted using a Gaussian line shape function with a fwhm of 15 cm^{-1}. For each cluster, the geometry, relative vibrational zero point energy (in kJ/mol), and IR spectrum of the global minimum isomer and of an energetically higher lying isomer is shown. Peaks are labeled according to their assignment to modes of the neutral acid molecule (**A**), of the conjugate base anion (**B**), or to shared proton stretching mode (**P**).

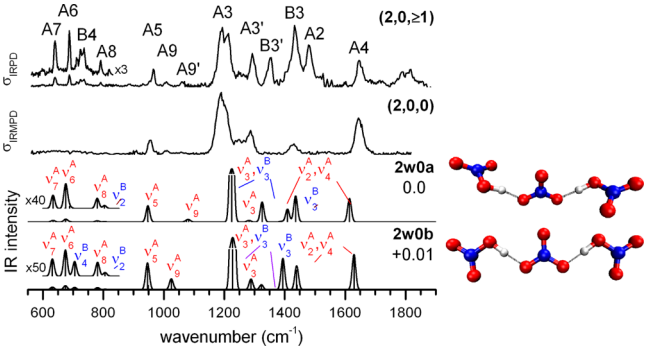

Figure 4. Experimental IRMPD and simulated linear absorption spectra of $NO_3^-(HNO_3)_2$ complexes, without (2,0,0) and with H_2-tagging (2,0,≥1). Simulated spectra, derived from B3LYP/aug-cc-pVTZ scaled (0.968) harmonic frequencies and intensities, are convoluted using a Gaussian line shape function with a fwhm of 15 cm^{-1}. The geometry, relative vibrational zero point energy (in kJ/mol), and IR spectrum of the two lowest energy isomers is shown. Experimental peaks and simulated vibrational modes (ν) are labeled according to their assignment to modes of the neutral acid molecule (**A**) or of the conjugate base anion (**B**). Note, for better visibility of the lower intensity features an axis break was used in plotting the predicted IR intensities.

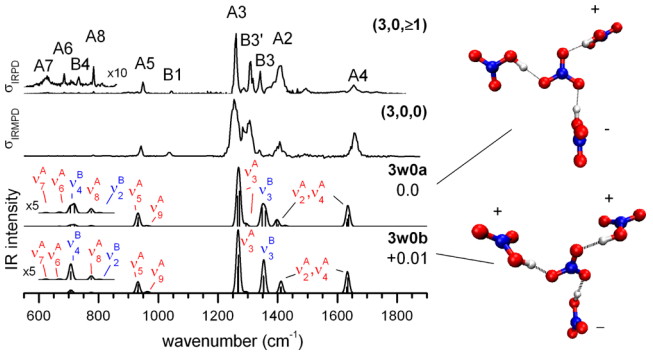

Figure 5. Experimental IRMPD and simulated linear absorption spectra of $NO_3^-(HNO_3)_3$ complexes, without (3,0,0) and with H_2-tagging (3,0, ≥1). Simulated spectra, derived from B3LYP/aug-cc-pVTZ scaled (0.968) harmonic frequencies and intensities, are convoluted using a Gaussian line shape function with a fwhm of 15 cm^{-1}. The geometry, relative vibrational zero point energy (in kJ/mol), and IR spectrum of the two lowest energy isomers is shown. Experimental peaks and simulated vibrational modes (ν) are labeled according to their assignment to modes of the neutral acid molecule (**A**) or of the conjugate base anion (**B**) (see Table 2). HNO_3 groups above the NO_3^--plane are denoted with +; those below are denoted with − (for details see text).

Table 3. Symmetry and Relative Energies (in kJ/mol) without (ΔE) and with Zero-Point-Energy Corrections (ΔE_{ZPE}) of the Lowest Energy B3LYP/aug-cc-pVTZ Minimum-Energy Structures for $NO_3^-(HNO_3)_m(H_2O)_n$ Clusters[a]

cluster	symbol	symmetry	ΔE	ΔE_{ZPE}
$NO_3^-(HNO_3)$	**1w0a**	C_S	0.0	0.0
	1w0b	C_1	0.2	0.1
$NO_3^-(HNO_3)(H_2O)$	**1w1a**	C_s	0.0	0.0
	1w1b	C_1	3.6	0.2
	1w1c	C_1	0.2	0.4
	1w1d	C_1	0.3	0.5
	1w1e	C_s	2.2	0.6
	1w1f	C_1	3.8	1.4
	1w1g	C_1	3.7	2.0
$NO_3^-(HNO_3)(H_2O)_2$	**1w2a**	C_1	0.0	0.0
	1w2b	C_s	1.4	0.1
	1w2c	C_s	2.4	0.2
	1w2d	C_1	3.0	1.0
	1w2e	C_s	4.3	1.5
	1w2f	C_s	4.3	1.5
	1w2g	C_1	4.3	1.6
	1w2h	C_1	5.3	2.2
	1w2i	C_1	6.8	8.4
$NO_3^-(HNO_3)_2$	**2w0a**	C_2	0.0	0.0
	2w0b	C_{2v}	0.4	0.0
	2w0c	C_1	0.2	0.2
	2w0d	C_s	0.6	0.6
	2w0e	C_s	1.3	1.1
$NO_3^-(HNO_3)_3$	**3w0a**	C_1	0.2	0.0
	3w0b	C_1	0.0	0.0
	3w0c	$C_1(C_3)$	1.0	0.8
	3w0d	C_{3h}	2.1	1.4

[a]See SI for a complete list of all isomers considered.

The delocalized nature of the calculated normal modes complicates their description. Therefore, we choose to assign the bands based on a comparison to the normal modes of the

dx.doi.org/10.1021/jp412222q | J. Phys. Chem. A 2014, 118, 7613−7622

individual moieties. These combinations of "localized" normal modes were identified qualitatively by eye. In several cases, significant mixing occurs between these modes, in particular, for the ${}^{A}\nu_2/{}^{A}\nu_4$ and ${}^{A}\nu_3/{}^{B}\nu_3$ pairs, introducing some ambiguity in our assignment.

***m* = 1/*n* = 0.** The two lowest energy structures **1w0a** and **1w0b** both exhibit the shared-proton motif $O_2NO^-\cdots H^+\cdots ONO_2^-$ (see Figure 3). The B3LYP/aug-cc-pVTZ global minimum energy structure **1w0a** is planar and has C_s symmetry. A first-order transition state of D_{2h} symmetry, connecting the two possible C_s isomers along the proton-transfer coordinate, is found only +0.2 kJ/mol higher in energy (see Table 3). Thus, while the minimum-energy structure is asymmetric with respect to the position of the proton in between the two nitrate moieties, inclusion of zero-point energy (zpe) is sufficient to overcome the barrier to proton transfer and this cluster effectively contains an equally shared proton. This effect is reflected in the relatively short O−O distance (r_{OO}) of the O···H$^+$···O moiety (2.45 Å), indicating the presence of short strong hydrogen bonds (SSHB).[52] In addition, a nonplanar isomer **1w0b** (C_1-symmetry) is also found only +0.2 kJ/mol higher in energy, with the corresponding first-order transition state (C_2-symmetry) at +0.3 kJ/mol relative to the C_s structure. Consequently, the potential energy hypersurface in the vicinity of the central proton is very flat with regard to proton transfer as well as to nonplanarity, and one thus expects a symmetrically delocalized proton combined with large amplitude motion of nitrate moieties already in the vibrational ground state. Pronounced anharmonic effects in the gas phase vibrational signature of strong hydrogen bonds are well documented,[16,53] and the following assignments are therefore only tentative in nature, but sufficient for our purpose. Performing anharmonic calculations on this system goes beyond the scope of the present study, but will be the focus of a follow-up paper.

The presence of both isomeric forms is needed to explain the experimental IRMPD spectra, a reasonable assumption given the low predicted barriers to isomerization. The simulated IR spectra of **1w0a** and **1w0b** (see Figure 3) are rather similar, differing mainly in the 1300−1500 cm^{-1} region. Both spectra exhibit extended mode-coupling of the shared proton stretching (${}^{P}\nu_x$) and bending (${}^{P}\nu_y$ and ${}^{P}\nu_z$) local modes with the nitrate local modes (${}^{B}\nu_{1-4}$) on each nitrate moiety; only the leading terms are indicated above each band in Figure 3. The intense band **P** (877 cm^{-1}) is assigned to the shared proton stretching mode ${}^{P}\nu_x$, but since this mode strongly couples to the NO symmetric stretching (${}^{B}\nu_1$) and NO_3 in-plane rocking (${}^{B}\nu_4$) modes, it also contributes to weaker bands **B1** (${}^{B}\nu_1$, ${}^{P}\nu_x$) and **B4** (${}^{B}\nu_4$, ${}^{P}\nu_x$). ${}^{P}\nu_x$ is predicted to red-shift considerably from the planar (919 cm^{-1}) to the nonplanar (868 cm^{-1}) isomer. Thus, isomerization between the two structures probably contributes significantly to the extended width of the shared proton band **P** (as well as all other bands). Combinations of the nitrate antisymmetric stretching modes (${}^{B}\nu_3$), which couple to the ${}^{P}\nu_{x,y}$ modes, are predicted around 1450 cm^{-1} and account for the **B3** bands. The planar isomer **1w0a** exclusively contributes to band **B3**, while **1w0b** also accounts for the satellite bands at lower (**B3′**) and higher energies (**B3″**). Notably missing from the experimental spectrum are the predicted bands above 1600 cm^{-1} and below 600 cm^{-1}, which we attribute to the inefficiency of the IRMPD process.[25,54] Note that these bands are recovered upon addition of a water molecule (see below), which lowers the dissociation limit of the cluster and thus reduces the number of absorbed photons required to induce dissociation.

***m* = 1/*n* = 1.** Two nearly iso-energetic, characteristically different binding motifs are predicted for the $m = 1$, $n = 1$ cluster. The global minimum energy structure (**1w1a**) is planar (C_s) with the water molecule bound to a single nitrate moiety in a double donor (DD) fashion (see Figure 3). A nonplanar (C_1) isomer (**1w1b**) containing a bridging DD water molecule is calculated +3.6 kJ/mol higher in energy, but the zpe-correction reduces the energy difference down to only +0.2 kJ/mol (see Table 3). The latter isomer is characterized by a shorter r_{OO} distance between the nitrate moieties (2.46 Å vs 2.52 Å; see Figure 3), indicating stronger central hydrogen bonds and leading to a more symmetric proton binding with O−H bond lengths of 1.12 Å and 1.34 Å, compared to 1.06 Å/1.46 Å in **1w1a**. At least five more isomers with similar water binding motifs are found within +2 kJ/mol (including zpe) of **1w1a** (see Table 3).

The simulated IR spectra of **1w1a** and **1w1b** (see Figure 3) are markedly different, reflecting the different water binding motif as well as the different hydrogen bond lengths involving the central proton. The IR spectrum of **1w1a** is characterized by a single intense band at 1226 cm^{-1} (${}^{A}\nu_3$, ${}^{B}\nu_3$), while the **1w1b** spectrum exhibits four similar intense bands at 1739 (${}^{P}\nu_x$, ${}^{P}\nu_y$), 1419 (${}^{B}\nu_3$, ${}^{P}\nu_y$), 1023 (${}^{B}\nu_1$, ${}^{P}\nu_x$), and 946 cm^{-1} (${}^{P}\nu_x$, ${}^{B}\nu_4$). Note that the normal modes of **1w1a** are better understood in terms of an asymmetric $NO_3^-\cdots(HNO_3)$ complex, while those of **1w1b**, which exhibits stronger central hydrogen bonds, reflect the shared proton motif. Satisfactory agreement with the experimental spectrum is only found for the **1w1b** spectrum, which predicts all observed bands (see Figure 3). Hence, the first water molecule adds to hydrogen dinitrate in a bridging fashion *without* significantly perturbing the SSHB.

***m* = 1/*n* = 2.** For $m = 1$, $n = 2$ a larger number of energetically low-lying, planar, and nonplanar isomers are found, seven within +2 kJ/mol (including zpe) of the global ground state, which only differ in how the water molecules bind to a hydrogen dinitrate core (see Table 3). The two lowest energy isomers contain an acceptor/donor/donor (ADD) bridging water molecule (see Figure 3), with the planar isomer **1w2b** minimally higher in energy (+0.1 kJ/mol) than the nonplanar **1w2a**. The next two isomers, **1w2c** (+0.2 kJ/mol, planar) and **1w2d** (+1.0 kJ/mol, nonplanar), contain DD waters that bind to the same nitrate moiety. These are followed by two isomers, **1w2e** (+1.5 kJ/mol, planar) and **1w2f** (+1.5 kJ/mol, nonplanar), which contain two DD water molecules, one of them in a bridging position. Isomers containing two bridging waters are found higher in energy (≥2.8 kJ/mol). Similar to the $m = 1/n = 1$ clusters, the central hydrogen bonds are strengthened by bridging water molecules, reflected in the dependence of r_{OO} on the presence of zero (**1w2c**: 2.56 Å), one (**1w2a**: 2.53 Å) and two (**1w2i**: 2.48 Å) bridging water molecules.

The simulated IR spectra of the six lowest energy isomers are all quite similar with three characteristic IR active modes of decreasing intensity at ∼1250 cm^{-1} (${}^{A}\nu_3$, ${}^{B}\nu_3$), ∼1400 cm^{-1} (${}^{B}\nu_3$, ${}^{A}\nu_2$, ${}^{A}\nu_4$), and ∼1600 cm^{-1} (${}^{A}\nu_2$, ${}^{A}\nu_4$, ${}^{H_2O}\nu_{bend}$). Compared to the experimental spectrum of (1,2,0), the predicted IR spectra of **1w2a** to **1w2d** fit equally well (see Figure 3 and SI), making an assignment to a particular water binding motif difficult. It is probable that multiple, interconverting isomers (with slightly different IR spectra) are present, accounting for the broad IR bands observed in the experimental spectra. The appearance of band **A5** and the intense band **A3** (see Figure 3), which are not observed in the experimental spectra of the smaller clusters, however, signals that solvation by two water molecules is sufficient to asymmetrically perturb the central SSHB.

dx.doi.org/10.1021/jp412222q | J. Phys. Chem. A 2014, 118, 7613−7622

***m* = 2/*n* = 0.** The most stable binding motif for the $m = 2$ clusters consists of a central nitrate moiety solvated by two nitric acid molecules. The global minimum energy structure is the nonplanar C_2-structure **2w0a** (see Figure 4). The planar C_{2v} structure **2w0b** is calculated +0.4 kJ/mol higher in energy, but inclusion of zpe reduces the energy difference to +0.01 kJ/mol. Three additional isomers with a similar binding motif (**2w0c-e**, see SI) lie within +1.1 kJ/mol (including zpe) of **2w0a** (Table 3).

All five structures **2w0a-e** yield similar IR spectra with the most notable differences in the 1300 to 1500 cm^{-1} region, where strongly coupled NO_2 symmetric ($^{A}\nu_3$) and antisymmetric ($^{A}\nu_2$) stretching, nitrate antisymmetric stretching ($^{B}\nu_3$), as well as NOH bending ($^{A}\nu_4$) modes are predicted. The simulated IR spectrum of **2w0b** fits particularly well (see Figure 4), because it reproduces the relative positions and intensities of bands **A2**-**A9**, **B3**, and **B4**. Only the relative intensity of the most intense peak at 1224 cm^{-1} ($^{A}\nu_3$, $^{B}\nu_3$), which corresponds to band **A3**, is apparently overestimated, but this is the case for all isomers. The spectrum of this isomer cannot account for the feature at ~1800 cm^{-1} or band **A9′** (see Figure 4). Band **A9′** can be nicely reproduced by considering the presence of a second isomer **2w0a**, whose H−O−NO torsion mode ($^{A}\nu_9$) is blue-shifted by +55 cm^{-1} compared to **2w0b**. The feature at ~1800 cm^{-1}, on the other hand, is not predicted in any of the simulated spectra. The OH stretching mode ($^{A}\nu_1$) is predicted at 2445 cm^{-1} and is therefore too high to account for this feature, so it is more likely due to combination bands.

***m* = 3/*n* = 0.** The lowest energy structures for the $m = 3$ clusters all contain a centrally solvated nitrate ion with three nitric acid molecules binding to the three terminal O-atoms. In the global minimum energy structure **3w0a** (see Figure 5), one of the nitric acid ligands lies nearly in the same plane as the nitrate ion, while the other two lie almost perpendicular to this plane. The corresponding N−O···H−O dihedral angles are 168°, 86°, and −87°. Consequently, the N-atoms of the three nitric acid units are arranged in-plane (in, ~180°), above (up, >0°), and below (down, <0°) the nitrate plane, and we refer to this arrangement as the in/up/down configuration. **3w0b**, also shown in Figure 5, exhibits an up/up/down configuration (94°/84°/−84°) and is calculated only +0.2 kJ/mol above **3w0a**. Inclusion of zpe makes these two conformers nearly isoenergetic (see Table 3). The symmetric (C_3) up/up/up (97°/97°/97°) conformer **3w0c** lies +1.0 kJ/mol (+0.8 kJ/mol) above **3w0a**. The planar in/in/in (180°/180°/180°) configuration of C_{3h} symmetry lies +2.1 kJ/mol above **3w0a** and is not a minimum on the potential energy surface, but rather a first-order transition state, indicating that the barriers to interconversion are small, similar to the smaller clusters.

The simulated IR spectra of the three lowest isomers (see Figure 5 and SI) all qualitatively reproduce the experimental IRMPD spectra. Bands **A2** to **A5** are assigned to modes predominantly involving the $^{A}\nu_{2-5}$ vibrations of the nitric acid ligands. Bands **B3** and **B3′**, separated by ~30 cm^{-1}, are tentatively attributed to the two components of the nitrate N═O antisymmetric stretch ($^{B}\nu_3$), signaling an asymmetric solvation environment. This splitting is seen particularly well in the H_2-tagged spectrum (3,0,≥1) in Figure 5, suggesting that messenger-tagging traps this conformer in a shallow local minimum. The IRMPD spectrum of the bare anion probes a somewhat hotter ion distribution, in which this effect is averaged out by rapid isomerization, and thus mainly a single band (**B3′**) is observed in this region. A splitting of 11 cm^{-1} is predicted for **3w0a**, three times smaller than the observed value. Band **B1** is attributed to the nitrate symmetric stretch ($^{B}\nu_1$), which is nominally IR-inactive in the bare nitrate ion, but obtains its IR intensity due to non-centrosymmetric solvation. Bands **A5**−**A8** are assigned to the N−O(H) stretching mode ($^{A}\nu_5$) as well as the nitric acid core bending modes $^{A}\nu_8$, $^{A}\nu_6$, and $^{A}\nu_7$, respectively, while band **B4** is the in-plane rocking mode of the nitrate core.

V. DISCUSSION

Equally Shared Proton Regime. The consideration of anharmonic effects in full dimensionality is essential for a quantitative description of the IR signature of prototypical systems containing SSHBs, as was recently shown for example for $H_5O_2^+$ and $H_3O_2^-$.[55,56] Hence, the apparent qualitative agreement of the predicted harmonic IR spectra of $H^+(NO_3^-)_2$ and $H^+(NO_3^-)_2(H_2O)$ with the experimental IRMPD spectra is interesting but possibly fortuitous. Therefore, it would be helpful to use another criterion to confirm our assignment of the shared proton stretching band (ν_x^p). For proton-bound heterodimers, one can estimate ν_x^p from the difference in proton affinity of the two groups.[53] Here, we propose that for proton-bound homodimers one may use the dependence of ν_x^p on the distance r of the (heavy) atoms sharing the proton, i.e., r_{OO} in the present case, as a criterion for the assignment of ν_x^p in the equally shared proton regime. Comparison of available gas phase values reveals that ν_x^p of $H^+(NH_3)_2$, $H^+(OH^-)_2$, $H^+(NO_3^-)$, and $H^+(H_2O)_2$ are 374 cm^{-1},[57] 697 cm^{-1},[58] 877 cm^{-1} (present work), and 1047 cm^{-1},[59] respectively, while the predicted values for r (for the equally shared proton configuration) are 2.75 Å,[57] 2.51 Å,[58] and 2.44 Å (present work, C_{2h} geometry), and 2.40 Å,[60] respectively. Hence, the vibrational frequency of the shared proton stretching mode *increases* monotonically with *decreasing* r in the equally shared proton regime. Simply put, stronger confinement of the motion of the shared proton along the internuclear (heavy atom) axis leads to an increase of the spacing of the vibrational levels and hence an increase of the fundamental vibrational transitions, supporting our assignment. This relationship should hold as long as the barrier for proton transfer is nonexistent or small compared to the zero-point energy.

Influence of Solvation. The central proton in hydrogen dinitrate sensitively responds to solvation with water or nitric acid molecules. Figure 6 shows calculated O−H bond lengths as a function of r_{OO}, which is a measure for the HB strength, for the relevant cluster geometries described above. The nonplanar conformer of hydrogen dinitrate (**1w0b**) exhibits the shortest O−O distance (2.44 Å), followed by its planar counterpart (**1w0a**: 2.46 Å). Addition of a single water molecule does not necessarily destabilize this arrangement if it binds in a bridging fashion (**1w1b**). However, if the water adds to a single nitrate moiety (**1w1a**) or two water molecules are added (**1w2a**, **1w2c**), then r_{OO} increases significantly (>2.52 Å) and the SSHB motif is replaced by a short covalent O−H and a longer HB. A more pronounced effect (2.57 Å) is observed upon addition of a second nitric acid molecule (**2w0a**, **2w0b**). Finally, the third nitric acid molecule completes the first solvation shell around the nitrate ion and exhibits the weakest ($r_{OO} \geq 2.62$ Å) HBs. Hand in hand with the softening of the SSHB, the N−O(H) bond lengths increase from 1.33 Å to 1.37 Å in the nitric acid units and decrease to 1.25 Å in the nitrate core.

The above-described softening of the SSHB, originally present in bare hydrogen dinitrate, upon solvation has several effects on its experimental IR signature. In the spectrum of the bare hydrogen dinitrate anion, the characteristic shared proton stretching mode is observed at 877 cm^{-1}. Addition of one

dx.doi.org/10.1021/jp412222q | J. Phys. Chem. A 2014, 118, 7613−7622

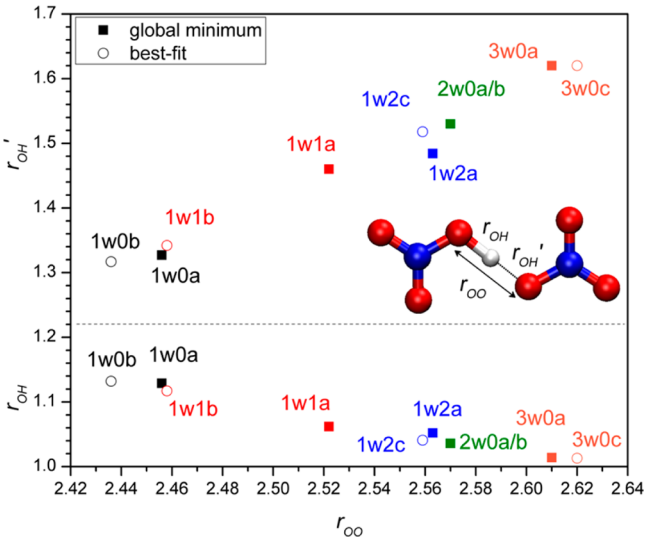

Figure 6. B3LYP/aug-cc-VTZ O−H bond lengths r_{OH} and r_{OH}' of the structures shown in Figures 3 to 5 as a function of the O−O distance r_{OO}. All distances are given in Å.

water molecule leads to a blue shift of 21 cm^{-1} in the IRMPD spectrum. Addition of more than one water molecule or nitric acid molecule moves it to higher energies and out of the investigated spectral range. Concomitant with the lifting of the symmetric binding arrangement, the characteristic IR active bands of nitric acid appear in the IR spectrum.

IRMPD Transparency. Upon messenger-tagging with H_2, bands emerge in the N═O stretching and core bend regions for the $m > 1$ clusters, which are not observed in the IRMPD spectra of the corresponding bare species. Moreover, the spectra of the H_2-tagged clusters are in much better agreement with the simulated linear absorption spectra predicted by the harmonic calculations. There are two reasons for this behavior. First, fewer photons are needed to photodissociate the H_2-anion complex, and hence the IRMPD intensities are closer to the linear absorption cross sections. Second, the H_2-anion complexes are colder, since the overall internal energy must lie close to or below the anion-H_2 bond dissociation energy for the tagged complex to survive. The observation of IRMPD transparent bands has been recently discussed in the context of hydrogen bond network disruption in sulfate−sulfuric acid clusters.[25] Here, the origin of the observed IRMPD transparency is different, as no hydrogen bonds can be broken in the bare cluster anions without immediate dissociation. Rather, in the present case, the large amplitude motion due to conformational fluctuations of the clusters already at low internal energies leads to a less efficient absorption IRMPD process. Presumably, this is a consequence of a "smearing out" of the transition strengths for the first few absorption steps, resulting in the absence of peaks in the IRMPD spectra of the hotter bare clusters compared to the single- or few-photon spectra of the colder H_2-tagged clusters.

VI. SUMMARY AND CONCLUSIONS

In summary, the present study reports the first IRMPD spectra of nitrate/nitric acid/water clusters in the fingerprint region. It shows that IRMPD is a sensitive method for probing the solvation environment and emphasizes the exceptional solvation behavior of the $m = 1$ cluster. While the addition of a single water molecule does not destabilize the shared proton motif, additional solvation is sufficient to induce an asymmetry in the central strong hydrogen bonds, leading to a solvated nitrate/nitric acid motif for the larger clusters. The change in solvation motif is reflected in the concomitant disappearance of the shared proton mode and the appearance of characteristic HNO_3 modes.

Similar to previously reported results for microsolvated conjugated base anions,[25,54,61] this work provides additional examples for systems with IRMPD transparent modes. Tagging with H_2 molecules or addition of water lowers the dissociation limit of the cluster such that this transparency is lifted or relaxed, leading to additional bands in the core bending and N═O stretching region. The tagged spectra are in much better agreement with the calculated frequencies and intensities.

Comparison of thin film results to the IRMPD spectra of the higher hydrated $m = 2$ clusters shows a strong resemblance to the condensed phase, suggesting that upon additional hydration the changes in nitric acid modes will be small. However, further spectroscopic experiments on microsolvated conjugate base anions are necessary to determine the degree of acid dissociation in $NO_3^-/HNO_3/H_2O$ clusters as a function of the cluster composition and temperature.

■ ASSOCIATED CONTENT

Supporting Information

Comparison of experimental IRMPD and additional simulated linear absorption spectra for $NO_3^-(HNO_3)_m(H_2O)_n$ clusters. Tabulated energies, symmetries, and geometrical parameters for minimum-energy structures.This material is available free of charge via the Internet at http://pubs.acs.org.

■ AUTHOR INFORMATION

Corresponding Authors

*E-mail: knut.asmis@uni-leipzig.de.
*E-mail: dneumark@berkeley.edu.

Notes

The authors declare no competing financial interest.

■ ACKNOWLEDGMENTS

We thank the Stichting voor Fundamenteel Onderzoek der Materie (FOM) for granting the required beam time and greatly appreciate the skill and assistance of the FELIX staff. This research is funded by the European Community's Seventh Framework Program (FP7/2007-2013, Grant 226716) and the Air Force Office of Scientific Research (FA9550-12-1-1060). T.I.Y. thanks the National Science and Engineering Research Council of Canada (NSERC) for a postgraduate scholarship.

■ REFERENCES

(1) Arnold, F. Atmospheric Ions and Aerosol Formation. *Space Sci. Rev.* **2008**, *137*, 225−239.
(2) Castleman, A. W.; Tang, I. N. Role of Small Clusters in Nucleation about Ions. *J. Chem. Phys.* **1972**, *57*, 3629−3638.
(3) Arnold, F.; Henschen, G. First Mass Analysis of Stratospheric Negative Ions. *Nature* **1978**, *275*, 521−522.
(4) Heitmann, H.; Arnold, F. Composition Measurements of Tropospheric Ions. *Nature* **1983**, *306*, 747−751.
(5) Viggiano, A. A.; Arnold, F. The First Height Measurements of the Negative Ion Composition of the Stratosphere. *Planet. Space Sci.* **1981**, *29*, 895−906.
(6) Beig, G.; Brasseur, G. Model of Tropospheric Ion Composition: A First Attempt. *J. Geophys. Res.* **2000**, *105*, 22671−22684.
(7) MacTaylor, R. S.; Castleman, A. W. . J. Cluster Ion Reactions: Insights into Processes of Atmospheric Significance. *J. Atmos. Chem.* **2000**, *36*, 23−63.

(8) Dunlap, B. I.; Robert J. Doyle, J. Ammonium Nitrate Cluster Ions. *J. Phys. Chem.* **1996**, *100*, 5281−5285.
(9) Galvez, O.; Gomez, P. C.; Pacios, L. F. Theoretical Study of Stratospheric Relevant Anions: Nitrate Nitric Acid Complexes. *J. Phys. Chem. A* **2006**, *110*, 3750−3758.
(10) Gillard, R. D.; Ugo, R. Adducts of Co-ordination Compounds. Part II. Compounds of Nitric Acid and Trans-dihalogeno-tetrapyridinemetal(III) Nitrates. *J. Chem. Soc.* **1966**, *A*, 549−552.
(11) Detoni, S.; Diop, L.; Gunde, R.; Hadzi, D.; Orel, B.; Potier, A.; Potier, J. Vibrational-Spectra and Structure of Complexes containing the Hydrogen. *Spectrochim. Acta, Part A* **1979**, *35*, 443−454.
(12) Emsley, J. Very Strong Hydrogen Bonding. *Chem. Soc. Rev.* **1980**, *9*, 91−124.
(13) Dobinson, G. C.; Mason, R.; Russell, D. R. The Structure of the Hydrogen Dinitrate Ion. *Chem. Commun. (London)* **1967**, 62−63.
(14) Gunde, R.; Solmajer, T.; Azman, A.; Hadzi, D. The Hydrogen Dinitrate Ion: I. Ab-Initio Calculation of Configuration and of Proton Potential Curve. *J. Mol. Struct.* **1975**, *24*, 405−408.
(15) Barlic, B.; Hadzi, D.; Orel, B. Normal Coordinate Analysis of the Two Forms of the Hydrogen Dinitrate Ion. *Spectrochim. Acta* **1981**, *37A*, 1047−1048.
(16) Asmis, K. R.; Neumark, D. M.; Bowman, J. M. Gas Phase Vibrational Spectroscopy of Strong Hydrogen Bonds. In *Gas Phase Vibrational Spectroscopy of Strong Hydrogen Bonds. In Hydrogen-Transfer Reactions*; Hynes, J. T., Klinman, J. P., Limbach, H.-H., Schowen, R. L., Eds.; Wiley-VCH: Weinheim, Germany, 2007; pp 53−78.
(17) Faithful, B. D.; Wallwork, S. C. The Structure of the Hydrogen Dinitrate Ion in Tetraphenylarsonium Hydrogen Dinitrate. *Chem. Commun. (London)* **1967**, 1211−1211.
(18) Roziere, J.; Lehmann, M. S.; Potier, J. Disordered Structure of an $O_2NOHONO_2^-$ ion. A Neutron Diffraction Study of Trans-dichlorotetrakis(pyridine)rhodium(III) hydrogendinitrate. *Acta Crystallogr., Sect. B: Struct. Sci.* **1979**, *35*, 1099−1102.
(19) Ahlijah, G. E. B. Y.; Mooney, E. F. The Attenuated Total Refelction Spectra of Ployatomic Inorganic Anions - II. The Nitrogen Containing Anions. *Spectrochim. Acta* **1969**, *25A*, 619−627.
(20) Waterland, M. R.; Kelley, A. M. Far-Ultraviolet Resonance Raman Spectroscopy of Nitrate Ion in Solution. *J. Chem. Phys.* **2000**, *113*, 6760−6773.
(21) Fehsenfeld, F. C.; Howard, C. J.; Schmeltekopf, A. L. Gas Phase Ion Chemistry of HNO_3. *J. Chem. Phys.* **1975**, *63*, 2835−2841.
(22) Lovejoy, E. R.; Bianco, R. Temperature Dependence of Cluster Ion Decomposition in a Quadrupole Ion Trap. *J. Phys. Chem. A* **2000**, *104*, 10280−10287.
(23) Lovejoy, E. R.; Curtius, J. Cluster Ion Thermal Decomposition (II): Master Equation Modeling in the Low-Pressure Limit and Fall-Off Regions. Bond Energies for $HSO_4^-(H_2SO_4)_x(HNO_3)_y$. *J. Phys. Chem. A* **2001**, *105*, 10874−10883.
(24) Sekimoto, K.; Takayama, M. Observations of Different Core Water Cluster Ions $Y^-(H_2O)_n$ (Y = O_2, HO_x, NO_x, CO_x) and Magic Number in Atmospheric Pressure Negative Corona Disspectrometryspectrometry. *J. Mass Spectrom.* **2010**, *45*, 50−60.
(25) Yacovitch, T. I.; Heine, N.; Brieger, C.; Wende, T.; Hock, C.; Neumark, D. M.; Asmis, K. R. Vibrational Spectroscopy of Bisulfate/Sulfuric Acid/Water Clusters: Structure, Stability and IRMPD Intensities. *J. Phys. Chem. A* **2013**, *117*, 7081−7090.
(26) Davidson, J. A.; Fehsenfeld, F. C.; Howard, C. J. The Heats of Formation of NO_3^- and NO_3^- Association Complexes with HNO_3 and HBr. *Int. J. Chem. Kinet.* **1977**, *9*, 17−29.
(27) Wlodek, S.; Luczynski, Z.; Wincel, H. Stabilities of Gas-Phase $NO_3^-(HNO_3)_n$, $n \leq 6$, Clusters. *Int. J. Mass Spectrom. Ion Phys.* **1980**, *35*, 39−46.
(28) Goebbert, D. J.; Garand, E.; Wende, T.; Bergmann, R.; Meijer, G.; Asmis, K. R.; Neumark, D. M. Infrared Spectroscopy of the Microhydrated Nitrate Ions $NO_3^-{}_3(H_2O)_{1-6}$. *J. Phys. Chem. A* **2009**, *113*, 7584−7592.
(29) Zhou, J.; Santambrogio, G.; Brümmer, M.; Moore, D. T.; Wöste, L.; Meijer, G.; Neumark, D. M.; Asmis, K. R. Infrared Spectroscopy of Hydrated Sulfate Dianions. *J. Chem. Phys.* **2006**, *125*, 111102.
(30) O'Brien, J. T.; Prell, J. S.; Bush, M. F.; Williams, E. R. Sulfate Ion Patterns Water at Long Distance. *J. Am. Chem. Soc.* **2010**, *132*, 8248−8249.
(31) Yacovitch, T. I.; Heine, N.; Brieger, C.; Wende, T.; Hock, C.; Neumark, D. M.; Asmis, K. R. Vibrational Spectroscopy of Atmospherically Relevant Acid Cluster Anions: Bisulfate versus Nitrate Core Structures. *J. Chem. Phys.* **2012**, *136*, 241102.
(32) Goebbert, D. J.; Meijer, G.; Asmis, K. R. 10K Ring Electrode Trap - Tandem Mass Spectrometer for Infrared Spectroscopy of Mass Selected Ions. *AIP Conf. Proc.* **2009**, *1104*, 22−29.
(33) Goebbert, D. J.; Wende, T.; Bergmann, R.; Meijer, G.; Asmis, K. R. Messenger-Tagging Electrosprayed Ions: Vibrational Spectroscopy of Suberate Dianions. *J. Phys. Chem. A* **2009**, *113*, 5874−5880.
(34) Oepts, D.; van der Meer, A. F. G.; van Amersfoort, P. W. The Free-Electron-Laser User Facility FELIX. *Infrared Phys. Technol.* **1995**, *36*, 297−308.
(35) Wende, T. *Gas Phase Infrared Photodissociation Spectroscopy of Mass-Selected Ionic Clusters: Metal Oxides and Microhydrated Anions*; Doctoral Thesis; Fachbereich Physik, Freie Universität Berlin, Germany.
(36) Gruene, P.; Lyon, J.; Fielicke, A. Vibrational Spectroscopy of Strongly Bound Clusters. In *Handbook of Nanophysics*; CRC Press, 2010, pp 1−14.
(37) *Turbomole v 6.2 2010*, a development of University of Karlsruhe and Forschungszentrum Karlsruhe GmbH, 1989−2007, Turbomole GmbH, since 2007; available from http://www.turbomole.com.
(38) Ahlrichs, R.; Bär, M.; Häser, M.; Horn, H.; Kölmel, C. Electronic Structure Calculations on Workstation Computers: The Program System Turbomole. *Chem. Phys. Lett.* **1989**, *162*, 165−169.
(39) Treutler, O.; Ahlrichs, R. Efficient Molecular Numerical-Integration Schemes. *J. Chem. Phys.* **1995**, *102*, 346−354.
(40) Becke, A. D. Density-Functional Exchange-Energy Approximation with Correct Asymptotic Behavior. *Phys. Rev. A* **1988**, *38*, 3098−3100.
(41) Becke, A. D. Density-Functional Thermochemistry. III. The Role of Exact Exchange. *J. Chem. Phys.* **1993**, *98*, 5648−5652.
(42) Lee, C.; Yang, W.; Parr, R. G. Development of the Colle-Salvetti Correlation-Energy Formula into a Functional of the Electron Density. *Phys. Rev. B* **1988**, *37*, 785−789.
(43) Kendall, R. A.; Thom H. Dunning, J.; Harrison, R. J. Electron Affinities of the First-Row Atoms Revisited. Systematic Basis Sets and Wave Functions. *J. Chem. Phys.* **1992**, *96*, 6796−6806.
(44) Deglmann, P.; Furche, F.; Ahlrichs, R. An Efficient Implementation of Second Analytical Derivatives for Density Functional Methods. *Chem. Phys. Lett.* **2002**, *362*, 511−518.
(45) Scott, A. P.; Radom, L. Harmonic Vibrational Frequencies: An Evaluation of Hartree-Fock, Moller-Plesset, Quadratic Configuration Interaction, Density Functional Theory, and Semiempirical Scale Factors. *J. Phys. Chem.* **1996**, *100*, 16502−16513.
(46) Halls, M. D.; Velkovski, J.; Schlegel, H. B. Harmonic Frequency Scaling Factors for Hartree-Fock, S-VWN, B-LYP, B3-LYP, B3-PW91 and MP2 with the Sadlej pVTZ Electric Property Basis Set. *Theor. Chem. Acc.* **2001**, *105*, 413−421.
(47) Marchand, P.; Marcotte, G.; Ayotte, P. Spectroscopic Study of HNO_3 Dissociation on Ice. *J. Phys. Chem. A* **2012**, *116*, 12112−12122.
(48) Barnes, A. J.; Lasson, E.; Nielsen, C. J. Molecular Complexes of Nitric Acid with Various Bases Studied by Matrix Isolation Infrared Spectroscopy. *J. Mol. Struct.* **1994**, *322*, 165−174.
(49) Irish, D. E.; Davis, A. R. Interactions in Aqueous Alkali Metal Nitrate Solutions. *Can. J. Chem.* **1968**, *46*, 943−951.
(50) McGraw, G. E.; Bernitt, D. L.; Hisatsune, I. C. Vibrational Spectra of Isotopic Nitric Acids. *J. Chem. Phys.* **1965**, *42*, 237−244.
(51) Relph, R. A.; Bopp, J. C.; Johnson, M. A.; Viggiano, A. A. Argon Cluster-Mediated Isolation and Vibrational Spectra of Peroxy and Nominally D_{3h} isomers of CO_3^- and NO_3^-. *J. Chem. Phys.* **2008**, *129*, 064305.
(52) Jeffrey, G. A. *An Introduction to Hydrogen Bonding*; Oxford University Press: New York, 1997.

(53) Roscioli, J. R.; McCunn, L. R.; Johnson, M. A. Quantum Structure of the Intermolecular Proton Bond. *Science* **2007**, *316*, 249−254.
(54) Yacovitch, T. I.; Wende, T.; Jiang, L.; Heine, N.; Meijer, G.; Neumark, D. M.; Asmis, K. R. Infrared Spectroscopy of Hydrated Bisulfate Anion Clusters: $HSO_4^-(H_2O)_{1-16}$. *J. Phys. Chem. Lett.* **2011**, *2*, 2135−2140.
(55) Vendrell, O.; Gatti, F.; Meyer, H.-D. Full Dimensional (15-Dimensional) Quantum-Dynamical Simulation of the Protonated Water Dimer. II. Infrared Spectrum and Vibrational Dynamics. *J. Chem. Phys.* **2007**, *127*, 184303.
(56) Pelaez, D.; Sadri, K.; Meyer, H.-D. Full-Dimensional MCTDH/MGPF Study of the Ground and Lowest Lying Vibrational States of the Bihydroxide Complex. *Spectrochim. Acta: Part A* **2014**, *119*, 42−51 Frontiers in Molecular Vibrational Calculations and Computational Spectroscopy..
(57) Yang, Y.; Kühn, O.; Santambrogio, G.; Goebbert, D. J.; Asmis, K. R. Vibrational Signatures of Hydrogen Bonding in the Protonated Ammonia Clusters $NH_4^+(NH_3)_{1-4}$. *J. Chem. Phys.* **2008**, *129*, 224302.
(58) Diken, E. G.; Headrick, J. M.; Roscioli, J. R.; Bopp, J. C.; Johnson, M. A.; Mccoy, A. B. Fundamental Excitations of the Shared Proton in the $H_3O_2^-$ And $H_5O_2^+$ Complexes. *J. Phys. Chem. A* **2005**, *109*, 1487−1490.
(59) Hammer, N. I.; Diken, E. G.; Roscioli, J. R.; Johnson, M. A.; Myshakin, E. M.; Jordan, K. D.; Mccoy, A. B.; Huang, X.; Bowman, J. M.; Carter, S. The Vibrational Predissociation Spectra of the $H_5O_3^+Rg_n$(RG = Ar, Ne) Clusters: Correlation of the Solvent Perturbations in the Free OH and Shared Proton Transitions of the Zundel Ion. *J. Chem. Phys.* **2005**, *122*, 244301.
(60) Ojamäe, L.; Shavitt, I.; Singer, S. J. Potential Energy Surfaces and Vibrational Spectra of H_5O Math Image and Larger Hydrated Proton Complexes. *Int. J. Quantum Chem. Symp.* **1995**, *29*, 657−668.
(61) Garand, E.; Wende, T.; Goebbert, D. J.; Bergmann, R.; Meijer, G.; Neumark, D. M.; Asmis, K. R. Infrared Spectroscopy of Hydrated Bicarbonate Anion Clusters: $HCO_3^-(H_2O)_{1-10}$. *J. Am. Chem. Soc.* **2010**, *132*, 849−856.
(62) Maki, A. G.; Wells, J. S. High-Resolution Measurement and Analysis of the Infrared Spectrum of Nitric Acid near 1700 cm^{-1}. *J. Mol. Spectrosc.* **1980**, *82*, 427−434.